Quantum Electronics **50** (1) 33–40 (2020)

https://doi.org/10.1070/QEL17207

Laser speckle contrast imaging of blood microcirculation in pancreatic tissues during laparoscopic interventions

E.V. Potapova, E.S. Seryogina, V.V. Dremin, D.D. Stavtsev, I.O. Kozlov, E.A. Zherebtsov, A.V. Mamoshin, Yu.V. Ivanov, A.V. Dunaev

Abstract. **Laser speckle contrast imaging of the microcirculatory bed of the pancreas is performed, which allows its condition to be assessed and thereby is an additional valuable tool for making a diagnostic decision and dynamically monitoring the effectiveness of the treatment for pathology of the abdominal organs. Laparoscopic operations on the pancreas are low-traumatic and in most cases avoid open surgical interventions. For the first time an experimental system for recording speckle images, combined with a commercially available five-millimetre rigid laparoscope, is presented. The sensitivity of the system to the fluid motion in a capillary at different velocities is determined, and the possibility of finding areas of blood microcirculation disturbance in modelling pancreatic ischemia in an experiment on laboratory animals is revealed. The laparoscope illumination channel is verified by comparison with speckle dynamics under external illumination of the studied object.**

Keywords: *laser speckle contrast imaging, laparoscopy, pancreas, ischemia, blood microcirculation.*

1. Introduction

Acute pancreatitis stably takes a leading place among acute surgical diseases of abdominal organs. The issues of diagnosis and treatment of this pathology continue to be ones of the most pressing problems of modern medicine. Acute pancreatitis in the early stages of the disease is accompanied by microcirculatory disorders in the pancreas, which are a key pathological process in the development of pancreatic necrosis [1]. Enzymatic autolysis and inflammation lead to vascular thrombosis of the microvasculature with the development of ischemia and pancreatic tissue necrosis [2]. This determines the relevance of assessing blood microcirculation in the tissues of the pancreas at the beginning of the disease and early detection of the destructive process, when there is a period of reversible pathological changes (ischemia and necrobiosis). In this regard, it is of interest to expand the capabilities of minimally invasive technologies, including laparoscopy, in assessing the state of pancreatic tissue, early diagnosis and treatment of various complications of acute pancreatitis.

At the present stage of the development of technologies used in medical diagnostics, optical methods for assessing the state of biological tissues have become widespread [3–6]. They are able to monitor microcirculatory disorders *in vivo* in real time with non-invasive or minimally invasive interventions. These include video microscopic methods: nail-fold [7, 8] and conjunctiva [9, 10] videocapillaroscopy, confocal and two-photon microscopy [11–13], orthogonal polarisation spectroscopy [14, 15] and dark-field spectroscopy [16, 17], optical coherence tomography [18, 19], as well as methods of dynamic light scattering: laser Doppler flowmetry, laser Doppler imaging, laser speckle contrast imaging (LSCI) [20–22], etc.

The LSCI technology has recently become widespread in research and clinical practice, showing high sensitivity to microcirculatory disorders in various biological tissues [23–28]. The LSCI method is based on the registration of a random speckle interference pattern, which is formed on a detector that collects light backscattered from the surface of tissue illuminated by coherent laser light [29, 30]. The movement of particles inside the illuminated medium causes a spatial inhomogeneity of the scattered light detected by the detector, and leads to a blurry image due to the averaging of the picture during the exposure time. Then the temporal and spatial statistics of the speckle structure are used to obtain information on the motion of scattering particles [in the study of microcirculation, the wavelengths are selected in the red and infrared (IR) spectral ranges to record the movement of red blood cells]. The advantages of LSCI include the ability to conduct non-contact measurements of microcirculatory disorders in real time and forming a two-dimensional image of perfusion of the desired area with good temporal and spatial resolution at a reasonable cost of instrumentation. LSCI results are not quantitative, but are expressed as luminous flux intensities and are converted in relative units of spatial, temporal or spatiotemporal speckle contrast to form perfusion images of the studied area.

To assess the microcirculation of blood of pancreatic tissues, laser Doppler flowmetry [31] and orthogonal polarisation spectroscopy [32, 33] were used as methods of non-invasive optical diagnostics. The disadvantages of these methods include their point measurements, high sensitivity to artefacts from movement and pressure on the tissue, and, in the case of orthogonal polarisation spectroscopy, the duration

E.V. Potapova, E.S. Seryogina, D.D. Stavtsev, I.O. Kozlov, A.V. Dunaev Research and Development Centre of Biomedical Photonics, Orel State University, ul. Komsomolskaya 95, 302026 Orel, Russia; e-mail: potapova_ev_ogu@mail.ru;
V.V. Dremin, E.A. Zherebtsov Research and Development Centre of Biomedical Photonics, Orel State University, ul. Komsomolskaya 95, 302026 Orel, Russia; Optoelectronics and Measurement Techniques Laboratory, University of Oulu, Finland, Oulu, Pentti Kaiteran katu 1, 90014;
A.V. Mamoshin Research and Development Centre of Biomedical Photonics, Orel State University, ul. Komsomolskaya 95, 302026 Orel, Russia; Orel Regional Clinical Hospital, Bulvar Pobedy 10, 302028 Orel, Russia;
Yu.V. Ivanov Central Tuberculosis Research Institute, Yauzskaya Alleya 2, 107564 Moscow, Russia; Federal Scientific and Clinical Centre for Specialised Types of Medical Care and Medical Technologies, Federal Medical-Biological Agency of Russia, Orekhovyi bulvar 28, 115682 Moscow, Russia

Received 27 November 2019
Kvantovaya Elektronika **50** (1) 33–40 (2020)
Translated by V.L. Derbov

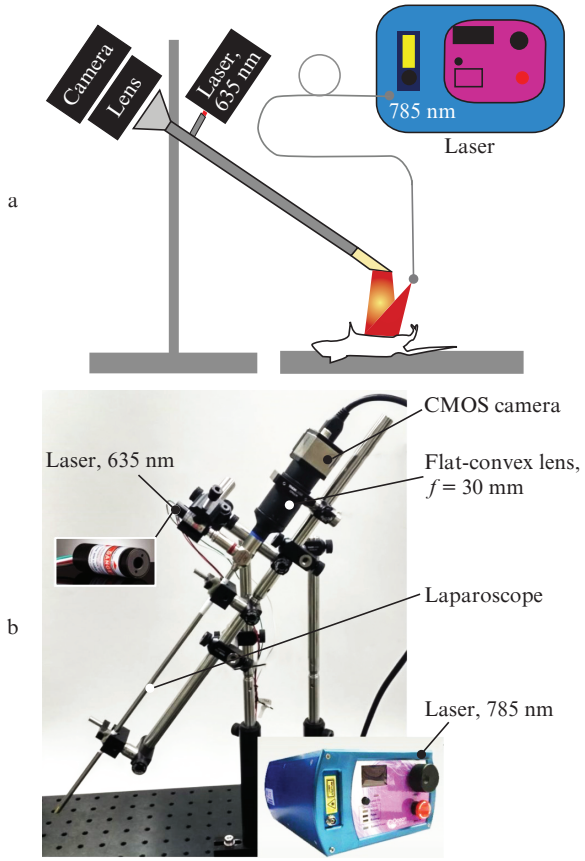

Figure 1. LSCI experimental system for intraoperative non-invasive monitoring of blood microcirculation during laparoscopic surgery: (a) schematic and (b) general appearance of the setup.

of the analysis of the obtained images. Despite the existing work on the use of LSCI in abdominal surgery in the study of liver microcirculation [34–38] and the gastrointestinal tract [39–42], there are very few studies using the method for recording microcirculatory disorders in pancreatic tissue [43, 44].

The integration of the LSCI method into standard laparoscopic techniques made it possible to image blood microcirculation in the rat retina [45], the inner ear of mice [46], the small [47] and large [48] intestines. Laparoscopic operations on the pancreas are less traumatic surgical interventions and allow one in most cases to avoid open surgical interventions, to reduce the length of hospital stay of patients, and to decrease the number of repeated operations and mortality. We failed to find published works on the combined use of LSCI and laparoscopy to monitor the state of blood flow in the pancreatic parenchyma. The aim of this work is to evaluate the possibility of using the LSCI method for intraoperative monitoring of blood microcirculation in pancreatic tissues during laparoscopic surgery.

2. Materials and methods

2.1. Laparoscopic speckle contrast laser imaging

To assess the possibility of monitoring blood microcirculation in pancreatic tissues during laparoscopic surgery, an experimental LSCI system was developed, combined with an optical five-millimetre rigid laparoscope (Richard Wolf GA-S001, Germany), the schematic and general appearance of which are shown in Fig. 1. The designed installation was rigidly fixed on a support.

To verify the proposed method for combining laparoscopic equipment and the LSCI method, we used two options for illuminating the surface of the test object with the laser light: through a standard laparoscope illumination channel and external illumination. In the first case, we used a 10 mW laser operating at a wavelength $\lambda = 635$ nm (Edmund Optics Inc., USA), and for external illumination, a laser source LASER-785-LAB-ADJ-FC (Ocean Optics, USA) with a light power of 20 mW and $\lambda = 785$ nm. This allowed a relatively comparable analysis of the lighting efficiency of the study area through the standard laparoscope channel. The use of different wavelengths and powers of light sources also made it possible to evaluate the effect of the depth of light penetration on the recorded signal.

The image was recorded using a DCC3260M CMOS camera (Thorlabs Inc., USA) with a resolution of 1936×1216 pixels and a pixel size of 5.86 μm. The image was projected onto the camera matrix through a plano-convex lens with a focal length $f = 30$ mm (Thorlabs Inc., USA). The image recording rate of the camera was 15 frames per second; the exposure time of the camera was 9 ms for all measurements. The original speckle images were transferred to a computer for further processing using an algorithm developed in the Matlab R2018b software environment and allowing a dynamic picture of speckle contrast changes to be recorded in real time.

Depending on the tasks, when processing speckle contrast images, spatial, temporal or spatiotemporal contrasts are calculated [49]. In this work, it was supposed to test the laparoscopic system according to a protocol with a change in blood flow over time. It is known that the spatial algorithm provides the best temporal resolution and, therefore, to assess the dynamics of changes in blood microcirculation, the contrast was calculated using the formula

$$K = \frac{\sigma_n}{\langle I \rangle_n}, \quad (1)$$

where n is the size of the calculation area; σ_n is the standard deviation of intensity; and $\langle I \rangle_n$ is the average intensity. The studies conducted earlier showed that for the LSCI spatial algorithm, the window size of 7×7 pixels ($n = 7$) is optimal between the spatial resolution and the accuracy of the estimated speckle contrast [30].

If moving scattering particles are present in the object illuminated by coherent light, then the blurring of the speckle image recorded by the camera will result in the observed standard deviation of the intensity being lower than for a completely static set of scatterers, and, therefore, the speckle image contrast will also be reduced. The average velocity of scattering particles is inversely proportional to the characteristic correlation time of the intensity of the observed speckle dynamics, τ_c. If the integration time of the camera, T, is much longer than the correlation time τ_c (for $\tau_c \leqslant 0.04T$), all changes in intensity will be averaged and the calculated contrast will tend to zero. Conversely, if the motion of scattering particles is minimal, so that $\tau_c \geqslant 4T$, the speckle image contrast will be maximum. Goodman [50] showed that in this case, under the most favourable conditions (using a single-frequency laser with a sufficiently long coherence time, linear polarisation, and ideally diffuse scattering medium), the

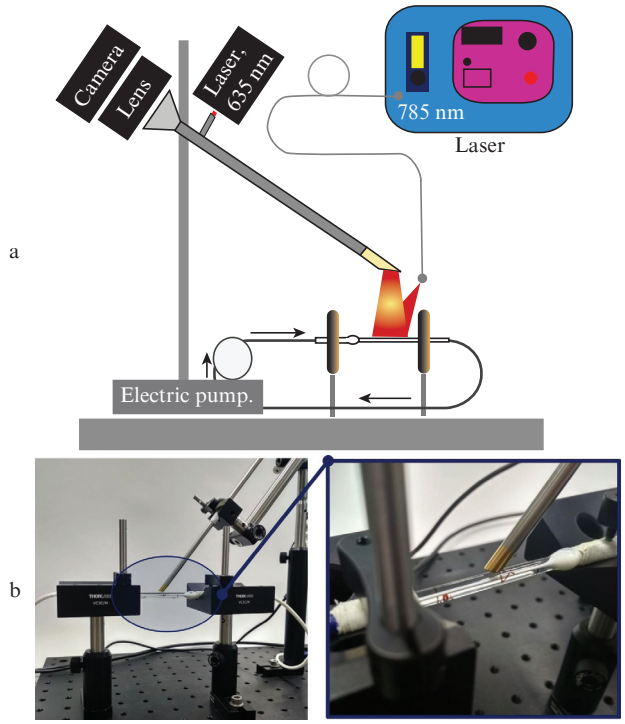

Figure 2. Setup for testing laparoscopic LSCI: (a) schematic and (b) general appearance of the setup.

observed standard deviation of the speckle image intensity tends to average intensity, and the speckle contrast approaches unity. The described behaviour of the speckle contrast value can be quantitatively analysed using the expanded expression for (1) [51]:

$$K = \frac{\sigma_n}{\langle I \rangle_n} = \left\{\beta\left\{\frac{\tau_c}{T} + \frac{\tau_c}{2T^2}\left[\exp\left(\frac{-2T}{\tau_c}\right) - 1\right]\right\}\right\}^{1/2}, \qquad (2)$$

where β is a constant depending on the parameters of the recording optics and the parameters of the sensor; and T is the exposure time.

Therefore, when the ratio τ_c/T varies from 10^{-2} to 10^{1}, the speckle contrast determined according to expression (2) will change between 0 and 1 in the form of a smooth S-shaped curve. Thus, the exposure time of 9 ms chosen in this work was considered optimal for the tested laparoscopic system, because it provides a sufficient amount of light incident on the camera matrix for both wavelengths. In addition, this parameter falls into the range [48] of the choice of exposure time when registering changes in the blood flow of laboratory animals using laser speckle contrast imaging.

To maximise the signal-to-noise ratio, the minimum speckle size must satisfy the Nyquist criterion [52]. Thus, the speckle size on the camera was adjusted by changing the pupil diameter of the laparoscopic system to achieve a speckle size of at least two times the pixel size. The speckle size was estimated using the technique from [52].

For visual analysis of the dynamics of the flow of scattering particles, the values of the calculated spatial contrast in the images were converted into pseudo colours, where the high velocity of the flow of scattering particles corresponded to red, and low, to blue.

2.2. Laser speckle contrast imaging of the motion of a scattering liquid in the capillary flow channel

To test the ability of the laparoscopic LSCI system to register the relative flow rates of scattering particles, a setup was assembled as described in [53], the schematic diagram and general appearance of which are shown in Fig. 2.

The setup consists of a capillary tube (inner diameter 1.6 mm), through which an 8% (by volume) solution of intralipid 20% (Fresenius Kaby, USA) was pumped using an electric pump calibrated by current/velocity. The selected 8% concentration of intralipid approximately corresponds to the optical scattering properties of blood at wavelengths of 635 and 785 nm [54, 55]. The camera recorded changes in the velocity of scattering particle motion in the capillary tube, and data post-processing was performed in accordance with formula (1). To test the LSCI system, the intralipid solution was passed through a capillary tube with linear velocities of 0, 0.5, 1, 1.5, and 2 mm s^{-1}, which covers the *in vivo* range of blood velocities in capillaries and arterioles, as well as the expected increase in velocities by a factor of 2–3 at the moment of reperfusion. The measurements were performed twice: when the capillary tube was illuminated with laser light at a wavelength of 635 nm through the standard illumination channel of the laparoscope and with external laser illumination at a wavelength of 785 nm. Since the selected velocity of the scattering liquid in the capillary exceeded the average velocity of the capillary blood flow, the frequency of recording images by the camera for this part of the experiment was 30 frames per second.

2.3. Pancreatic *in vivo* studies

The object of the study was a clinically healthy sexually mature laboratory rat Wistar (male) of three months of age with an initial body weight of 200 g. The experimental studies were carried out in accordance with the principles of good laboratory practice GLP (according to GOST 33647-2015). The work was approved by the ethics committee of Orel State University (protocol No. 12 dated 6 September 2018). The animal was kept in quarantine controlled for temperature, humidity and purity for two weeks. During the experiment, the animal was placed on a special fixing platform in a supine position. A transverse laparotomy was made for each animal and access was provided to the upper section of the posterior wall of the abdominal cavity in the retroperitoneal space. The organocomplex containing the pancreas was separated and placed on a laboratory table. Then the body of the pancreas stood out and a ligature of polyester filament was imposed above it, compressing the feeding vessel. Additionally, a cotton swab dipped in a 0.9% sodium chloride solution was placed in the surgical field. After that, the animal was placed under the optical system to visualise the studied area and record sequences of frames (see Fig. 1a). At the end of the study, the animal was withdrawn from the experiment in accordance with the rules of the experiments.

The vascular occlusion test is a classic test to assess microvascular function and, after an ischemic period, leads to an increase in microvascular blood flow as a result of reperfusion. Transient pancreatic ischemia was achieved by varying degrees of compression of the vessels supplying the pancreas. The ligature overlay scheme is shown in Fig. 3.

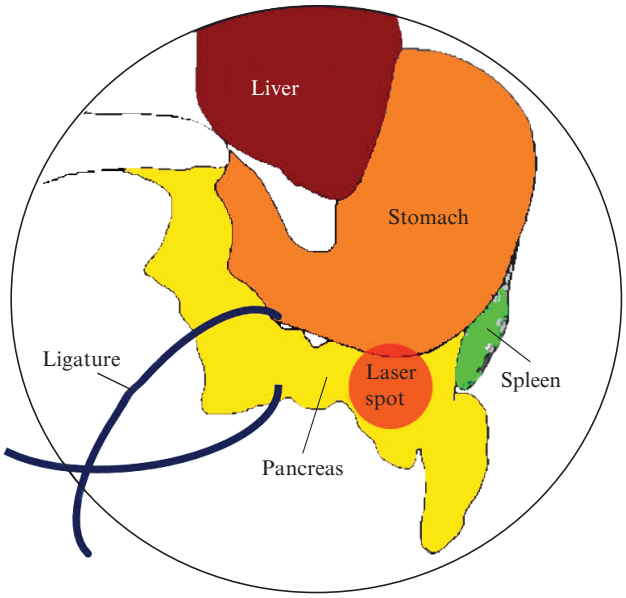

Figure 3. Ligature overlay scheme.

The experimental protocol consisted of several stages:

1. Basic test, 1 min, recording LSCI in series of 30 s with sequential illumination of the surface of the pancreas with laser light with $\lambda = 635$ and 785 nm with basic blood flow.

2. Mild ligation for 3 min, recording LSCI at $\lambda = 635$ nm for 30 s, starting from the 2nd minute from the start of the procedure, recording LSCI at $\lambda = 785$ nm (30 s) after 2.5 min.

3. Medium ligation for 3 minutes, recording LSCI at $\lambda = 635$ nm (30 s), starting from the 2nd minute, and recording LSCI at $\lambda = 785$ nm (30 s) after 2.5 min.

4. Reperfusion, accompanied by hyperaemia, for 1 min, recording LSCI at $\lambda = 635$ nm (30 s) from the start of the procedure and recording LSCI at $\lambda = 785$ nm (30 s) starting from the 30th second.

Between the main stages, work with ligature thread was carried out, which took no more than 1.5 minutes.

The methodology of the LSCI experiment on blood microcirculation in modelling pancreatic ischemia is illustrated in Fig. 4.

3. Experimental results and discussion

To record speckle images, the objects of study (capillary tube with a solution of intralipid and the pancreas of a rat) were placed under a laparoscope so that the studied area was in the focus of the laparoscope, which was controlled by the experimenter using a camera image.

To check the sensitivity of the setup to changes in the flow rate of scattering particles, we analysed a sequence of ten-second records for each of the five cases when the fluid moved through the tube at a velocity of 0, 0.5, 1, 1.5, and 2 mm s^{-1}. Processing of the data was carried out according to the spatial algorithm described above; speckle contrast images of the fluid motion in the capillary at various flow velocities are presented in Fig. 5.

For statistical processing, a region of 40×40 pixels (about 0.5 mm^2) in the central part of the tube was selected and the value of the spatial speckle contrast K was calculated using formula (1). The dependence of K on the velocity of the fluid along the capillary v is shown in Fig. 6.

In the absence of directed movement of the intralipid, speckle contrast does not tend to unity due to the small Brownian motion of the intralipid relative to the motionless walls of the capillary. There is a jump of K between the velocity $v = 0$ and $v = 0.5$ mm s^{-1}, but then K begins to linearly depend on v with determination coefficients of 0.96 and 0.94, when the capillary is illuminated by laser light with wavelengths of 635 and 785 nm, respectively.

Analysing the obtained data, we can conclude that the proposed experimental system for registering speckle images,

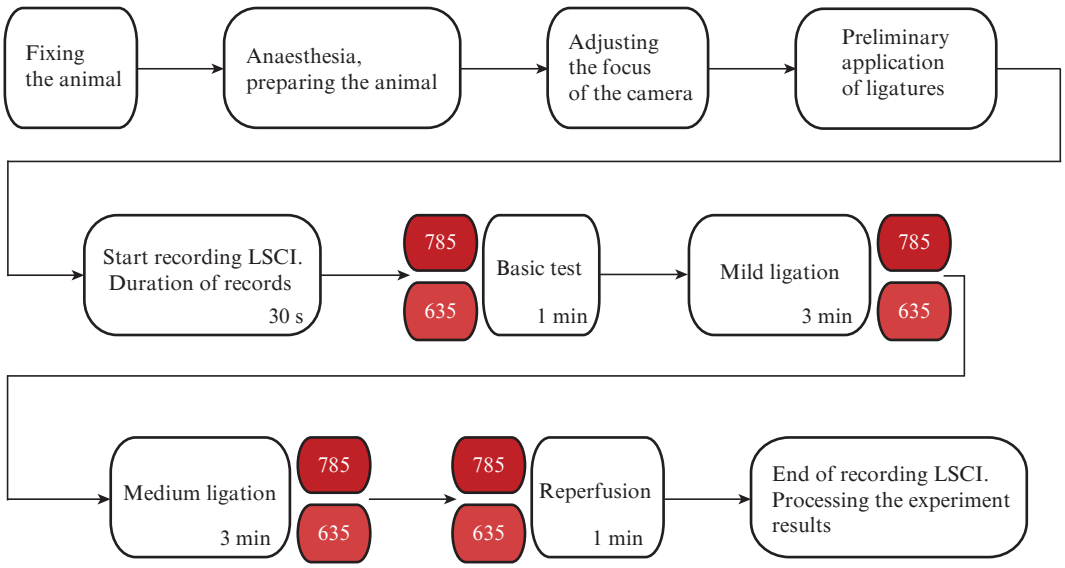

Figure 4. Methodology of the experiment on modelling pancreatic ischemia.

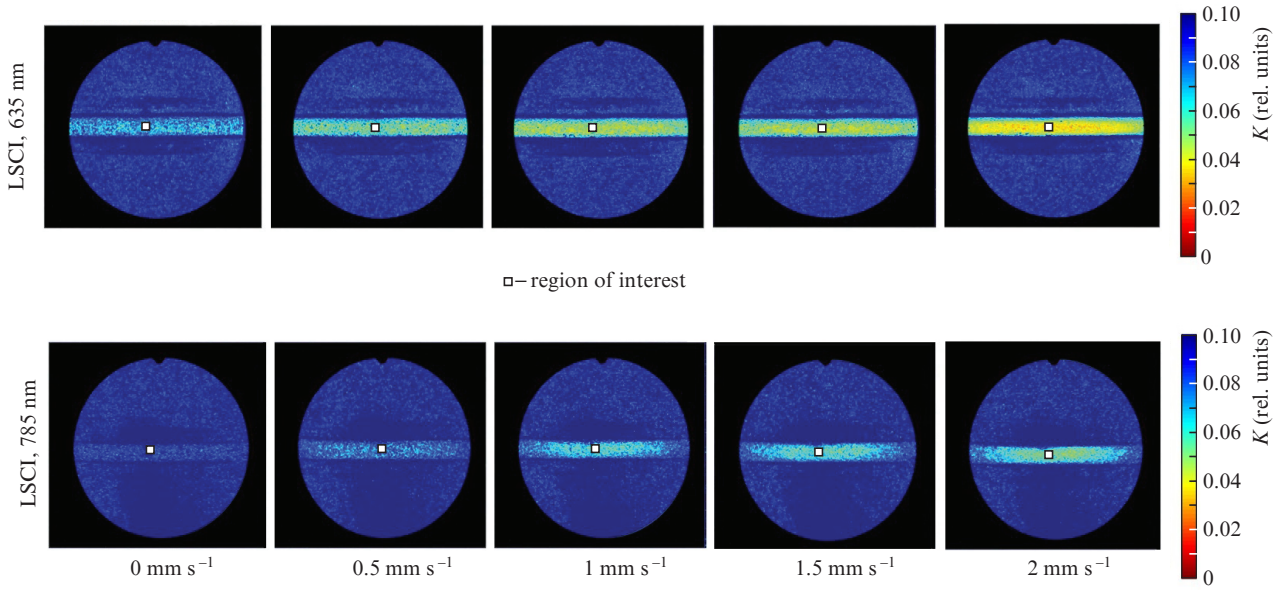

Figure 5. Speckle contrast images of fluid motion in a capillary at various flow velocities.

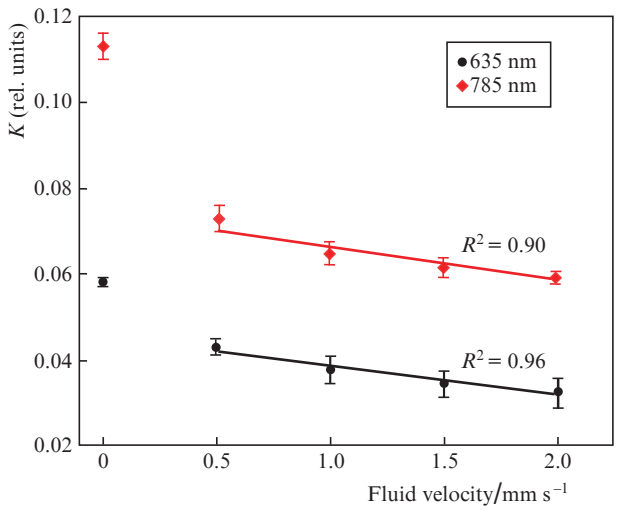

Figure 6. Dependences of spatial speckle contrast on the velocity of a liquid in a capillary. A linear relationship is shown by non-zero flow velocity.

combined with a commercially available laparoscope, provides a high-quality and clear indication of the change in flow in the capillary when simulating four different flow velocities selected within the range of velocities in vessels of the microvasculature.

Next, studies were conducted of dynamic changes in the blood flow of the rat pancreas. Figure 7 shows the image of the pancreas obtained on the camera of the laparoscopic system in white light mode, as well as the first frames of speckle contrast images processed by the spatial algorithm for each stage of the experimental protocol at two wavelengths.

In the visual analysis of the obtained images, a significant change in the speckle pattern during the period of medium ligation and reperfusion can be noted, and this is observed both when illuminated through the illumination channel of the laparoscope at $\lambda = 635$ nm, and under external illumination at $\lambda = 785$ nm.

To process the results of all stages of the experiment on the rat pancreas, we selected an area of interest (marked with a white square in Fig. 7) measuring 40×40 pixels (about 0.5 mm^2). The speckle contrast values for each frame were averaged over space. For further statistical processing, the vector of speckle contrast values was averaged over each stage. During the ligation, there was a slight displacement of the pancreas; therefore, during the processing, the experimenter determined the boundaries of interest at each stage, guided by the anatomical structures, in order to maximise the immutability of the analysed area.

For objective comparison of the experimental results under different lighting conditions, the data of each stage were normalised to the average speckle contrast calculated in the basic test. Figure 8 shows the results of statistical processing of the data of the relative contrast change at different stages of the experiment in the form of span diagrams, in which the centre line is the median and the box edges are the lower and upper quartiles (25th and 75th). The significance of statistical differences in speckle contrast, calculated in the area of interest of the pancreas at different stages of the protocol, was evaluated using one-way analysis of variance (one-way ANOVA). A value of $p < 0.01$ was considered significant.

Both in the case of using the illumination channel of a laparoscope and in case of external illumination of pancreatic tissue, a sequential change in the degree of ischemia at the 2nd and 3rd stages of the experiment is reflected in the graphs by a sharp stepwise increase in the value of speckle contrast. After the ligature removal, there is a significant decrease in speckle contrast, which corresponds to the notion of reactive hyperaemia in the organ during reperfusion and is consistent with previously published results obtained by the LSCI method for ischemia of different durations and subsequent reperfusion in the pancreas [56]. The results of our studies also correlate with few published data on the introduction of the LSCI method in laparoscopic techniques for the study of

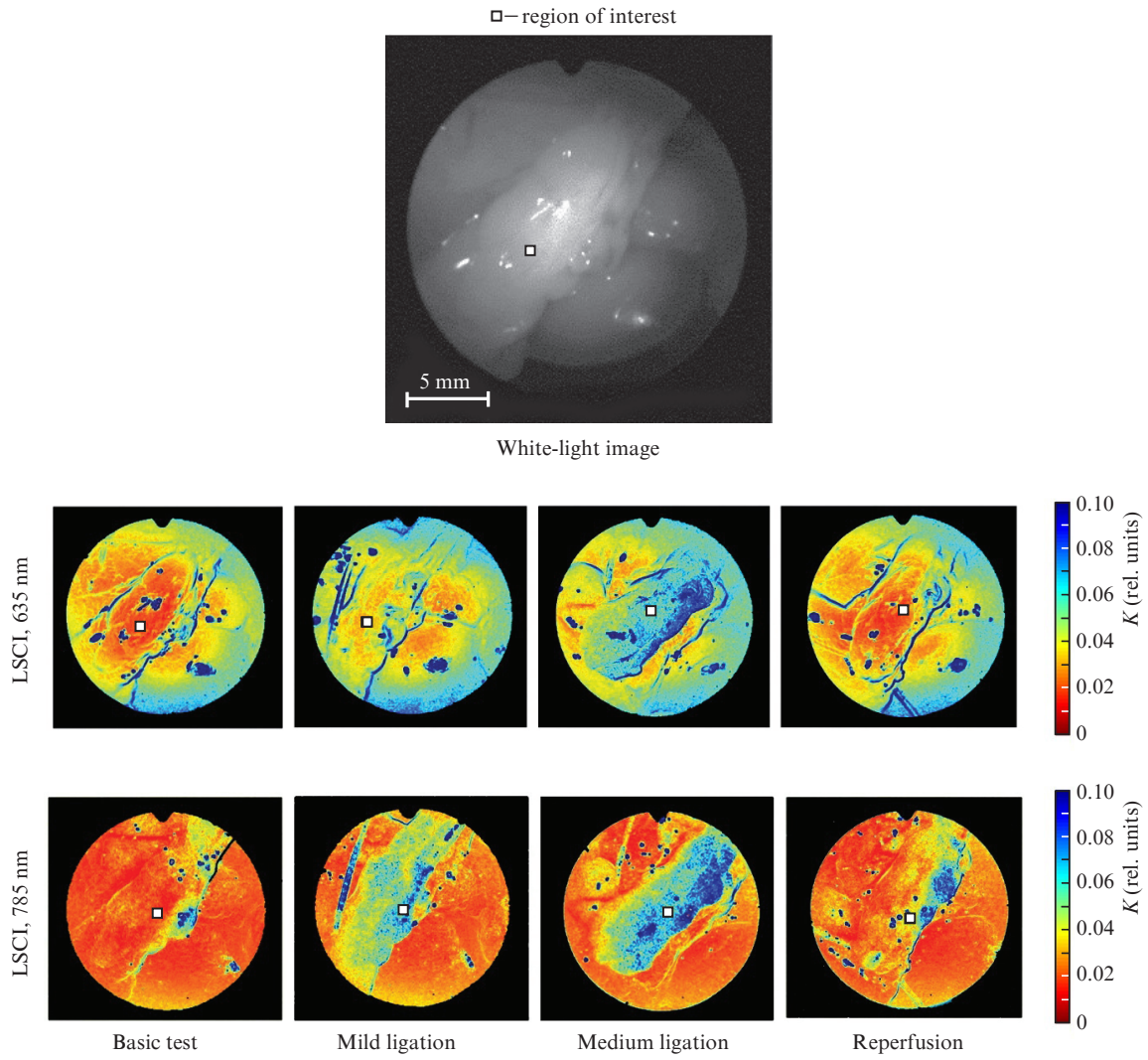

Figure 7. Image of the pancreas obtained on the camera of the laparoscopic system in white light mode and speckle contrast images obtained during the study of microcirculation of the blood of the pancreas at various stages of the protocol.

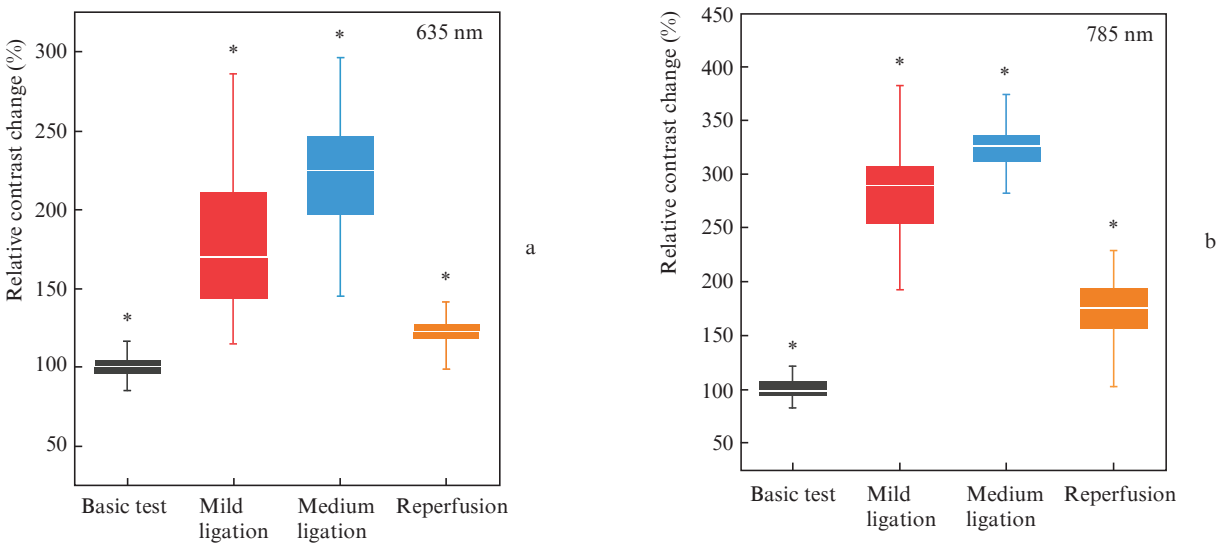

Figure 8. Spatial speckle contrast calculated in the region of interest of the pancreas at various stages of the protocol for (a) $\lambda = 635$ nm and (b) 785 nm. The statistical significance of the differences with respect to the previous stage of the protocol with a probability $p < 0.01$ is indicated by an asterisk.

perfusion of various organs. Zheng et al. [47] described an integrated laparoscopic speckle laser system that showed good sensitivity to changes in rat intestinal perfusion when modelling ischemia, as well as blood flow in the intestines, abdominal wall, and gall bladder in pigs. A similar work was published by Heeman et al. [48], which showed the possibility of imaging perfusion using laparoscopic LSCI and also described an occlusion test to check the sensitivity of the system to changes in blood flow in the large intestine. However, the use of laparoscopic techniques for visualising blood flow in the pancreas was carried out for the first time, we also proposed for the first time to use external illumination of the object of study with laser light at $\lambda = 785$ nm to verify the luminous channel of the laparoscope.

The observed discrepancy between the relative (normalised) changes in spatial contrast, when the pancreas is illuminated with laser light at $\lambda = 635$ nm through the standard illumination channel of the laparoscope and with external laser illumination with $\lambda = 785$ nm, can be explained by the peculiarities of the interaction of these wavelengths with biological tissue, as well as by different power of optical laser light. Hence, Fig. 8b demonstrates a more pronounced quantitative change in the relative speckle contrast between the stages of the experiment for $\lambda = 785$ nm, which may be associated with the probing of a larger volume of pancreatic biological tissue and, as a consequence, a greater number of microvessels. However, even with such differences, a similarity of reactions between the calculated parameter – spatial speckle contrast – to changes in blood microcirculation in the studied biological tissue is clearly observed. Thus, the obtained data show that the experimental system for recording speckle images, combined with a commercially available five-millimetre rigid laparoscope, is able to determine the areas of pancreatic blood microcirculation disturbance.

It is worth noting that the study has limitations. Thus, in the presented work, the instrument was rigidly fixed on the platform; thereby, we deliberately reduced the influence of an inherent disadvantage of the LSCI method, its sensitivity to motion artefacts. In addition, we did not compare our results with the results obtained using other methods of measuring blood microcirculation. To introduce the presented method of laparoscopic LSCI into clinical practice, it is planned to improve the software to increase the resistance to motion of artefacts, improve instrumentation implementation, including the introduction of polarisers in the circuit to reduce specular reflection, correct optical aberrations of various nature, and determine the resolution of the system. One of the possible ways to solve the problem of the influence of motion of artefacts on the signal may be to switch to high-speed cameras and shorter exposure times, which will make it possible to implement a high-speed protocol for registering speckle structures. In addition, the use of crossed polarisers in the circuit will make it possible to increase the sensitivity of the system to the relative velocity of the scattering centres by eliminating single scattering.

4. Conclusions

The paper presents an experimental system for recording speckle images combined with a commercially available five-millimetre rigid laparoscope, which extends the diagnostic capabilities of minimally invasive technologies in pancreatic surgery. It was shown that the device has good sensitivity to changes in the blood microcirculation of the studied area. Despite the limitations of the study (rigid fixation of the instrument on the platform and the absence of a reference method for the study of blood microcirculation), the possibility of using laser speckle contrast imaging of blood microcirculation in pancreatic tissues during laparoscopic interventions was shown for the first time. Real-time evaluation of tissue perfusion will expand the capabilities of minimally invasive technologies, including laparoscopy, in assessing the state of pancreatic tissue, early diagnosis and treatment of various complications of acute pancreatitis.

Acknowledgements. The study was supported by the Russian Science Foundation (Project No.18-15-00201).

References

1. Cuthbertson C.M., Christophi C. *Br. J. Surg*., **93**, 518 (2006).
2. Podoluzhnyi V.I. *Fundamental'naya i Klinicheskaya Meditsina*, **2**, 62 (2017).
3. Tuchin V.V. *Opticheskaya biomeditsinskaya diagnostika* (Optical Biomedical Diagnostics) (Moscow: Fizmatlit, 2007) Vol. 1, p. 560.
4. Lal C., Leahy M.J. *Microcirculation*, **23**, 345 (2016).
5. Sturesson C., Nilsson J., Eriksson S. *Med. Devices Evid. Res*., **7**, 445 (2014).
6. Rubins U., Marcinkevics Z., Cimurs J., Saknite I., Kviesis-Kipge E., Grabovskis A. *Biosensors.*, **9**, 97 (2019).
7. Dremin V., Kozlov I., Volkov M., Margaryants N., Potemkin A., Zherebtsov E., Dunaev A., Gurov I. *J. Biophotonics*, **12**, e201800317 (2019).
8. Gallucci F., Russo R., Buono R., Acampora R., Madrid E.L., Uomo G. *Adv. Med. Sci*., **53**, 149 (2008).
9. Cheung A.T., Hu B.S., Wong S.A., Chow J., Chan M.S., To W.J., Li J., Ramanujam S., Chen P.C. *Clin. Hemorheol. Microcirc*., **51**, 77 (2012).
10. Safonova T.N., Lutsevich Ye.E., Kintyukhina N.P. *Vestnik Oftal'mologii*, **132**, 90 (2016).
11. Cinotti E., Gergelé L., Perrot J.L., Dominé A., Labeille B., Borelli P. Cambazard F. *Ski. Res. Technol*., **20,** 373 (2014).
12. Ihler F., Bertlich M., Weiss B., Dietzel S., Canis M. *Biomed Res. Int. Hindawi Limited*, **2015**, 154272 (2015).
13. Huang J., Li L., Wang H., Liu S., Lu Y., Liao M., Tao R., Hong L., Fukunaga K., Chen Z., Wilcox C.S., Lai E.Y., Han F. *CNS Neurosci. Ther*., **20**, 816 (2014).
14. Cerný V., Turek Z., Parízková R. *Physiol. Res*., **56**, 141 (2007).
15. van Zijderveld R., Ince C., Schlingemann R.O. *Graefe's Arch. Clin. Exp. Ophthalmol*., **252**, 773 (2014).
16. Goedhart P.T., Khalilzada M., Bezemer R., Merza J., Ince C. *Opt. Express*, **15**, 15101 (2007).
17. Sha M., Griffin M., Denton C.P., Butler P.E. *Microvasc. Res*., **126**, 103890 (2019).
18. Kirillin M., Motovilova T., Shakhova N. *J. Biomed. Opt*., **22**, 1 (2017).
19. Gao W. *Microcirculation*, **25**, e12375 (2018).
20. Cracowski J.-L., Roustit M. *Microcirculation*, **23**, 337 (2016).
21. Mizeva I., Zharkikh E., Dremin V., Zherebtsov E., Makovik I., Potapova E., Dunaev A. *Microvasc. Res*., **120**, 13 (2018).
22. Sdobnov A., Bykov A., Molodij G., Kalchenko V., Jarvinen T., Popov A., Kordas K., Meglinski I. *J. Phys. D: Appl. Phys*., **51**, 155401 (2018).
23. Forrester K.R., Tulip J., Leonard C., Stewart C., Bray R.C. *IEEE Trans. Biomed. Eng*., **51**, 2074 (2004).
24. Kazmi S.M., Richards L.M., Schrandt C.J., Davis M.A., Dunn A.K. *J. Cereb. Blood Flow Metab*., **35**, 1076 (2015).
25. Agafonov D.N., Timoshina P.A., Vilenskiy M.A., Fedosov I.V., Tuchin V.V. *Izv. Sarat. Univer., Novaya Ser. Ser. Fiz*., **11**, 14 (2011).
26. Parthasarathy A.B., Weber E.L., Richards L.M., Fox D.J., Dunn A.K. *J. Biomed. Opt*., **15**, 066030 (2010).
27. Gnyawali S.C., Blum K.M., Pal D., Ghatak S., Khanna S., Roy S., Sen C.K. *Sci. Rep. Nature Publ. Group*, **7**, 41048 (2017).

28. Kalchenko V., Sdobnov A., Meglinski I., Kuznetsov Yu., Molodij G., Harmelin A. *Photonics*, **6**, 80 (2019).
29. Briers J.D. *Physiol. Meas*., **22**, R35 (2001).
30. Boas D.A., Dunn A.K. *J. Biomed. Opt*., **15**, 011109 (2010).
31. Liu M., Zhang X., Li B., Wang B., Wu Q., Shang F., Li A., Li H., Xiu R. *J. Vis. Exp*., **8**, e56028 (2018).
32. Schaser K., Puhl G., Vollmar B., Menger M.D., Stover J.F., Köhler K., Neuhaus P., Settmacher U. *Am. J. Transplant*., **5**, 341 (2005).
33. von Dobschuetz E., Biberthaler P., Mussack T., Langer S., Messmer K., Hoffmann T. *Pancreas*, **26**, 139 (2003).
34. Eriksson S., Nilsson J., Lindell G., *Sturesson C. Med. Devices*, **7**, 257 (2014).
35. Sturesson C., Milstein D.M., Post I.C., Maas A.M., van Gulik T.M. *Microvasc. Res*., **87**, 34 (2013).
36. Li C.H., Ge X.L., Pan K., Wang P.F., Su Y.N., Zhang A.Q. *Microvasc. Res*., **110**, 14 (2017).
37. Wu Y., Ren J., Zhou B., Ding C., Chen J., Wang G., Gu G., Liu S., Li J. *Microvasc. Res*., **97**, 137 (2015).
38. Ding C., Ren J., Zhou B., Wu Y., Shao X., Wang G., Fang J., Li J. *Microvasc. Res*., **95**, 26 (2014).
39. Milstein D.M., Ince C., Gisbertz S.S., Boateng K.B., Geerts B.F., Hollmann M.W., van Berge Henegouwen M.I., Veelo D.P. *Medicine* (*Baltimore*), **95**, e3875 (2016).
40. Ambrus R., Svendsen L.B., Secher N.H., Rünitz K., Frederiksen H.J., Svendsen M.B., Siemsen M., Kofoed S.C., Achiam M.P. *Scand. J. Gastroenterol*., **52**, 455 (2017).
41. Jansen S.M., de Bruin D.M., van Berge Henegouwen M.I., Bloemen P.R., Strackee S.D., Veelo D.P., van Leeuwen T.G., Gisbertz S.S. *Dis. Esophagus*, **31**, doy031 (2018).
42. Kojima S., Sakamoto T., Nagai Y., Matsui Y., Nambu K., Masamune K. *Surg. Innov*., **26**, 293 (2019).
43. Vilenskii M.A., Aleksandrov D.A., Timoshina P.A., Tuchin V.V., Skorokhod A.A., Yarovoi A.S. *Meditsina Ekstremal'nykh Situatsii*, **44**, 28 (2013).
44. Timoshina P., Bucharskaya A., Alexandrov D., Tuchin V. *J. Biomed. Photon. Eng*., **3**, 020301 (2017).
45. Ponticorvo A., Cardenas D., Dunn A.K., Ts'o D., Duong T.Q. *J. Biomed. Opt*., **18**, 090501 (2013).
46. Kong T.H., Yu S., Jung B., Choi J.S., Seo Y. *J. PLoS One*, **13**, e0191978 (2018).
47. Zheng C., Lau L.W., Cha J. *Biomed. Opt. Express*, **9**, 5962 (2018).
48. Heeman W., Dijkstra K., Hoff C., Koopal S., Pierie J.P., Bouma H., Boerma E.C. *Biomed. Opt. Express*, **10**, 2010 (2019).
49. Draijer M., Hondebrink E., van Leeuwen T., Steenbergen W. *Lasers Med. Sci*., **24**, 639 (2009).
50. Goodman J.W., in *Laser Speckle and Related Phenomena*. Ed. by J.C. Dainty (Berlin, Heidelberg: Springer, 1963, Topics Appl. Phys.) Vol. 9.
51. Briers D., Duncan D.D., Hirst E., Kirkpatrick S.J., Larsson M., Steenbergen W., Steenbergen W., Thompson O.B. *J. Biomed. Opt*., **18**, 066018 (2013).
52. Kirkpatrick S.J., Duncan D.D., Wells-Gray E.M. *Opt. Lett*., **33**, 2886 (2008).
53. Lal C., Banerjee A., Sujatha N.U. *J. Biomed. Opt*., **18**, 111419 (2013).
54. Aernouts B., Van Beers R., Watté R., Lammertyn J., Saeys W. *Opt. Express*, **22**, 6086 (2014).
55. Bosschaart N., Edelman G.J., Aalders M.C., van Leeuwen T.G., Faber D.J. *Lasers Med. Sci*., **29**, 453 (2014).
56. Aleksandrov D.A., Timoshina P.A., Tuchin V.V., Maslyakova G.N., Palatova T.V., Sedov D.S., Izmailov P.P. *Saratovskii Nauchno-meditsinskii Zh*., **12**, 106 (2016).